ORIGINAL PAPER

The application of multi-walled carbon nanotubes modified pencil graphite electrode for voltammetric determination of favipiravir used in COVID-19 treatment
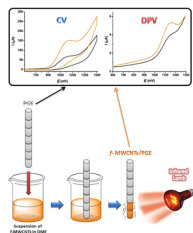
Serkan Karakaya[1] · Yusuf Dilgin[1]

Abstract

This study describes the first application of an improved procedure on a pencil graphite electrode decorated with functionalized multi-walled carbon nanotubes (*f*-MWCNTs/PGE) for the determination of the COVID-19 antiviral drug, favipiravir (FVP). The electrochemical behavior of FVP at f-MWCNTs/PGE was examined by cyclic voltammetry and differential pulse voltammetry (DPV) methods, and it was noted that the voltammetric response significantly increased with the modification of *f*-MWCNTs to the surface. The linear range and limit of detection from DPV studies were determined as 1–1500 μM and 0.27 μM, respectively. In addition, the selectivity of the method was tested toward potential interferences, which can be present in pharmaceutical and biological samples, and it was found that *f*-MWCNTs/PGE showed high selectivity for the determination of FVP in the presence of probable interferences. The results with high accuracies and precisions from the obtained feasibility studies also revealed that the designed procedure can be used for accurate and selective voltammetric determination of FVP in real samples.

Graphical abstract

Keywords Electrochemistry · Favipiravir · Functionalized multi-walled carbon nanotubes · Sensors voltammetry

Introduction

The coronavirus disease, known as coronavirus 2 (SARS-CoV-2), which manifests itself with acute respiratory syndrome, is a very dangerous viral disease [1]. SARS-CoV-2 (aka COVID-19), which first appeared in Wuhan, China, on December 2019, still affects the world through its various variants such as Omicron, Delta, and Ba.2–5 [2]. This viral disease manifests itself with mild symptoms and also causes serious diseases such as multi-organ failure, arrhythmias, shock, kidney and heart failure in advanced stages resulting in death [2]. COVID-19 caused a pandemic declaration by the World Health Organization (WHO) in March 2020 due to a major public health emergency [3]. The WHO reported that approximately 6.9 million people have died up to now due to this disease [4]. The pandemic necessitates an urgent solution in terms of treatment, and since the development of a new drug and the investigation of its effect on COVID-19 require months or years, prescription drugs with approved safety were preferred to be used in the first place [5]. One

✉ Serkan Karakaya
   skarakaya@comu.edu.tr

1 Chemistry Department of Science Faculty, Çanakkale
   Onsekiz Mart University, Çanakkale, Turkey

of these drugs, FVP, is a purine analog and RNA-dependent polymerase inhibitor and has been used in the treatment of COVID-19 viral infection [6]. The main advantages of FVP are that it is available in high doses and is very safe for use in patients [7]. The dosage of FVP is a significant issue in COVID-19 treatment, as inappropriate dosage may cause toxic or sub-therapeutic concentrations without apparent clinical benefit [8, 9]. Therefore, there is always an urgent need to develop reliable, sensitive, low-cost, and rapid analytical methods for the determination of FVP [1].

Convincing analytical methods for the determination of antiviral drugs for the treatment of COVID-19 are recommended not only for conventional quality control but also for the analysis of biological samples and pharmacokinetic studies [6]. In this term, many methods, such as high-performance liquid chromatography [10], spectrofluorimetry [11], and UV–Vis spectrophotometry [12], have been successfully used in the determination of FVP. However, these classical analytical techniques are often not easily accessible and require costly instruments, toxic solvents, and difficult and time-consuming sample preparation steps [13, 14]. Among these methods, electrochemical methods have received great attention due to their ease of use, high sensitivity, and low cost [1, 2, 6]. Therefore, it is recommended to develop sensitive, selective, and cost-effective electroanalytical procedures for the estimation of FVP in human plasma [15]. In this context, many studies on the electrochemical determination of FVP have recently been reported [1–3, 6, 9, 16–18].

Among the carbon-based electrodes, pencil graphite electrodes (PGEs) attract great attention due to their ease of availability, disposability, smaller background current, high sensitivity, low cost, and practicality in modification compared to the other traditional carbon electrodes such as carbon paste electrode (CPE) and glassy carbon electrode (GCE) [19–22]. Due to their unique properties, there is an increasing demand for the use of PGEs in the preparation of electrochemical sensors [23–31]. However, the voltammetric determination of an electroactive analyte at a bare electrode can be difficult due to poisoning by the adsorption of organic materials to the electrode surfaces [32]. Generally, modification of the electrode surfaces seems to be a good option to overcome these limitations by improving the electron transfer on the electrode surface and reducing the over potential [33]. In this connection, nanomaterials have been used in the preparation of the modified electrodes, and these materials provide an increase in the electrical, physical, and sensing performances of electrochemical sensors and improve selectivity and sensitivity [34]. One of the nanomaterials, carbon nanotubes (CNTs) has gained great attention due to their good electronic, chemical, thermal, mechanical, and geometric properties. Moreover, the modification of the electrode surfaces with CNTs increases the electrochemical reactivity and electrocatalytic effect due to

the edge plane-like imperfect structure of the CNTs [35]. Because of all their useful features, CNT-modified electrodes have been extensively used to detect a wide variety of analytes such as tramadol [36], aceclofenac [37], avanafil, doxorubicin [38], and acyclovir [39].

The aim of this study was to design of a practical, low-cost, selective, and sensitive electrochemical procedure for the determination of FVP at easily prepared *f*-MWCNTs/ PGE. Although bare PGE [2] and Tb nanoparticles@polytrihydroxybenzene composite modified PGE (TbNPs@ poly m-THB/PGE) [15] have already been used in the electrochemical determination of FVP, the electrochemical determination of FVP with the use of MWCNTs and PGE together has not been performed yet. The acidic functionalization of MWCNTs provides a large number of carboxyl and hydroxyl groups on the surface of MWCNTs, which increases the active sites of MWCNTs and improves the electrochemical response and selectivity [40]. The novelty of this study relies on the first use of *f*-MWCNTs and PGE together for the voltammetric determination of the COVID-19 drug, FVP. The results confirmed that the proposed methodology may enable the determination of FVP in real samples such as tablet formulations and biological samples with high accuracy and precision.

Results and discussion

Characterization studies

The cyclic voltammograms (CVs) and electrochemical impedance (EI) curves of the solution containing 5.0 mM $Fe(CN)_6^{3-/4-}$ redox couple were recorded for the electrochemical characterization studies (Fig. 1). When the CVs recorded at PGE are examined, the oxidation and reduction peaks of the redox couple can be seen. After *f*-MWCNTs were modified on the PGE surface, the current densities (I_a and I_c) of these peaks distinctly increased (Fig. 1A). EI spectroscopy is a very useful method to examine the surface conductivity properties of electrodes. The EI Nyquist chart consists of the following two parts: a semicircular region and a linear region. The semicircular part represents the charge transfer resistance (R_{ct}) at higher frequencies, and the linear portion is related to the lower frequencies corresponding to diffusion [41]. When the semicircular parts were examined, R_{ct} (60 Ω) measured for PGE significantly decreased to 36 Ω after the modification of *f*-MWCNTs (Fig. 1B). The changes observed in CVs and EI curves can be attributed to the good electrical conductivity properties, large and specific surface areas, and strong adsorptive abilities of MWCNTs [42, 43].

Surface characterizations of the electrodes were performed by recording SEM images of the electrodes (Fig. 3C and D). When the images are examined, the
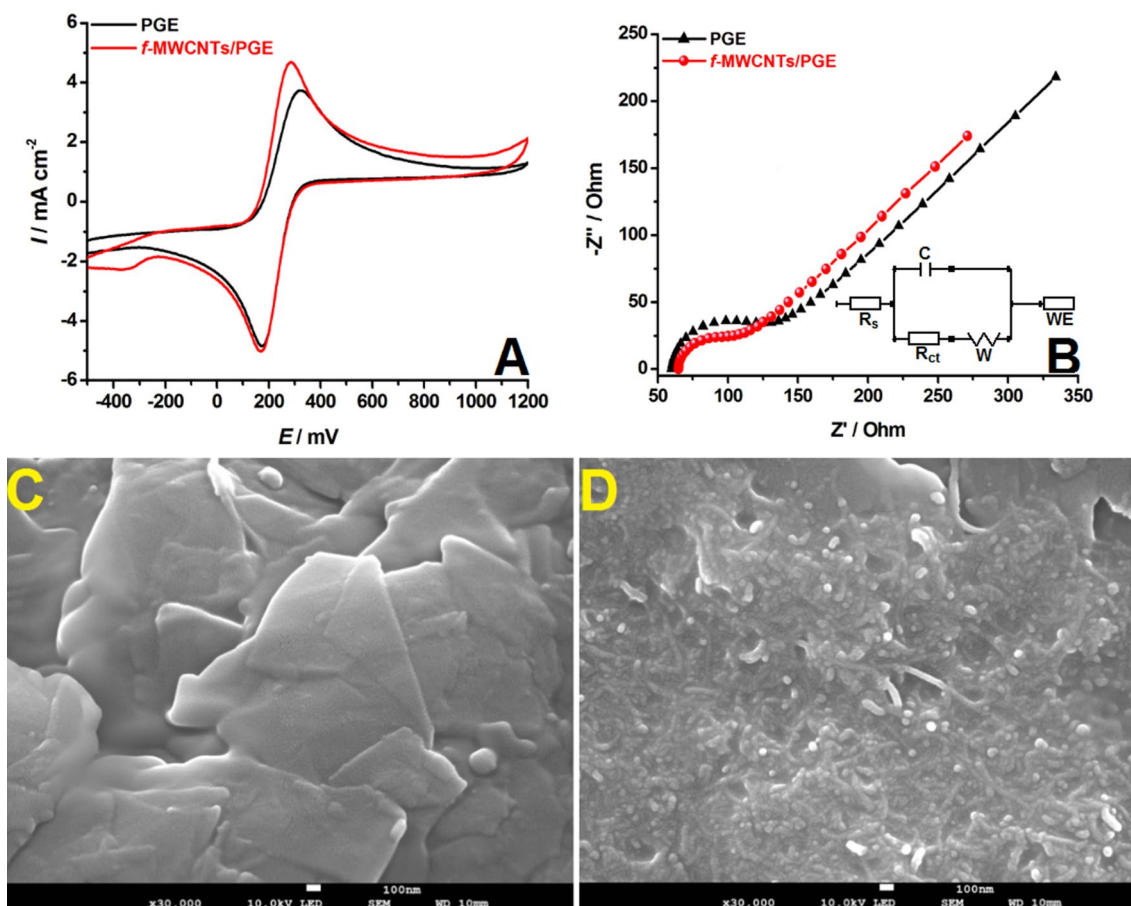
Fig. 1 **A** CVs of 5.0 mM Fe(CN)$_6^{3-/4-}$ + 0.1 M KCl solution recorded at PGE and *f*-MWCNTs/PGE (scan rate: 50 mV/s and potential range: −500 mV - 1200 mV) and **B** EI curves (frequency range: 100,000–0.10 Hz and inset is circuit model, WE: working electrode, R_s: ohmic resistance, *C:* double layer capacitance, *W:* Warburg impedance, SEM images (100 nm × 30,000) recorded at **C** PGE, and **D** *f*-MWC-NTs/PGE

surface morphology of the PGE is observed as smooth plates. After the modification process, *f*-MWCNTs homogeneously dispersed to the surface almost without agglomeration, and a certain change was observed in the surface morphology. In conclusion, the results from the characterization studies confirm the modification of *f*-MWCNTs on the PGE surface.

To investigate the effective surface area (ESA), the CVs for both electrodes were recorded at various scan rates ($v = 10$–500 mV s^{-1}) in a 5.0 mM Fe(CN)$_6^{3-/4-}$ solution containing 0.10 M KCl. The linear relationship was examined in the I_a vs. $v^{1/2}$ plots. The slopes for PGE and *f*-MWCNTs/PGE were found to be 4.82×10^{-4} and 5.38×10^{-4} A/(V s^{-1})$^{-2}$, respectively. According to the Randles–Sevcik Eq. (1) (I_p: peak current (A), *n*: number of the electrons, *A*: ESA (cm^2), C_0: concentration of Fe(CN)$_6^{3-/4-}$ (5.0×10^{-6} mol cm^{-3}), D: diffusion coefficient for Fe(CN)$_6^{3-/4-}$ (7.6×10^{-6} cm^2 s^{-1})) [2], the ESAs of the PGE and *f*-MWCNTs/PGE were calculated as 0.0507 and 0.0566 cm^2, respectively. In su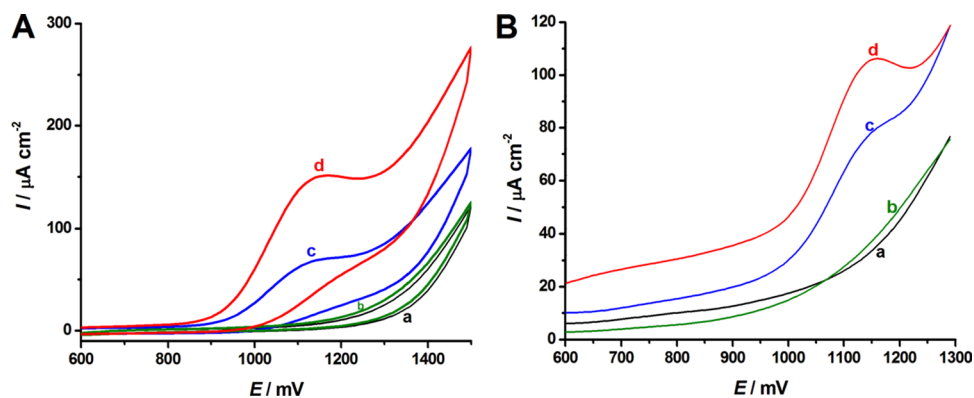mmary, the *f*-MWCNTs provide more ESA than bare PGE due to their good conductivity properties and large electroactive sites.

$$I_p = 2.69 \times 10^5 \times n^{3/2} \times A \times C_0 \times D^{1/2} \times v^{1/2} \tag{1}$$

Investigation of the electrochemical behavior of FVP

The electrochemical behavior of FVP was investigated by CV and DPV methods. Figure 2A reflects the CVs recorded for 0 mM (a,b) and 4.0 mM (c,d) FVP at PGE (a,c) and *f*-MWCNTs/PGE (b,d). As can be seen from the CVs, the electrochemical oxidation of FVP takes place at bare PGE, giving a weak peak at + 1.14 V. On the other hand, it was noted that the response increased approximately three times compared to the bare electrode without any significant change in peak potential. Similar results were also obtained for the recorded DPVs (Fig. 2B). The high voltammetric responses observed at the modified electrode have been attributed to the acceleration of electron transfer between

FVP and PGE due to the good conductivity properties and large active surface areas of the *f*-MWCNTs.

Investigation of the pH effect on the electrochemical behavior of FVP

To determine the most suitable supporting electrolyte for the electrochemical determination of FVP, CVs of 4.0 mM FVP at *f*-MWCNTs/PGE were recorded in BRBS with pH ranging from 3 to 8 (Fig. 3A). When the CVs are examined, it is seen that the oxidation peak potential (E_a) of FVP shifted in a less positive direction with the increase in pH. This shows that proton (H$^+$) plays a role in the electrochemical oxidation of FVP [16]. Moreover, the peak current appeared to increase gradually at pH 3 to 6, but a significant decrease in voltammetric response was observed at higher pH values (pH > 6). The decrease in response suggests that the hydrolysis and adsorption of FVP on the electrode surface may have decreased at higher pH values (Fig. 3B). In addition, the E_a is not dependent on pH at less acidic conditions (pH > 6), and this situation also indicates that H$^+$ transfer is not involved before the electron transfer rate-determination step at higher pH values. Therefore, the pH value of 6 with the highest voltammetric response was determined to be the most suitable supporting electrolyte.

The plots of E_a–pH produced from CVs are given together with the linear equation (E_a(V) = − 0.047 × pH + 1.3915 and R^2 = 0.9995) (Fig. 3C). The slope (0.047 V/pH), calculated from the equation is near the Nernstian value (0.059), indicates that the equivalent numbers of protons (H$^+$) and electrons (e$^-$) play a role in the oxidation of FVP at the electrode surface [17].

Scan rate effect on the electrochemical behavior of FVP

The scan rate (*v*) effect on the response of FVP was tested by recording the CVs of a pH 6 BRBS solution containing 4.0 mM FVP at different scan rates (Fig. 4A). As seen

from the CVs, E_a shifts towards more positive values, and I_a is enhanced by the increase of "*v*" which confirms the irreversible reaction on the electrode surface [44]. More-over, the high-linearity relationship between I_a and $v^{1/2}$ (I (μA) = 1.0756 × $v^{1/2}$ + 16.9426 and R^2 = 0.9983) shows that the oxidation of FVP at the *f*-MWCNTs/PGE sur-face occurs in a diffusion controlled process (Fig. 4B) [1]. The slope (~ 0.42) calculated from the Log*I*–Log*v* plots (Log*I* = 0.4155 × Log*v* + 1.0432 and R^2 = 0.9912) near the value of 0.5 also proves the diffusion-controlled oxidation of FVP on the electrode surface (Fig. 4C) [45]. The number of electrons involved in the oxidation of FVP was deter-mined using the Laviron Eq. (2), where k_s is the constant of electron transfer rate, R is the constant of molecular gas (8.314 J mol^{-1} K^{-1}), T is temperature as 298.15 K and F is faraday constant as 96,485 C mol^{-1} [46]. For this pur-pose, the linearity relationship in the E_a – ln*v* plots produced from the recorded CVs was emphasized by the line equation E_a(V) = 0.0297 × ln*v* + 1.0515 (R^2 = 0.9983) (Fig. 4D). When the calculated slope was taken into consideration, α × n was calculated as 0.87 (2), where "α" is the electron transfer coefficient, and it is generally accepted as $\alpha = 0.5$ for irre-versible electrode reactions [3]. Therefore, the n value was calculated as 1.74, and the number of electrons involved in the redox process at the *f*-MWCNTs/PGE was found to be $n \approx 2$.

$$E_a = E° + \left(\frac{RT}{anF}\right) \ln \left(\frac{RTk_s}{anF}\right) + \left(\frac{RT}{anF}\right) \ln v \qquad (2)$$

Differential pulse voltammetric determination of FVP

DPVs of increasing concentrations of FVP at bare and modified electrodes under optimum conditions were recorded to determine FVP (Fig. 5A and B). The lin-ear relationship is expressed by the calibration plots for
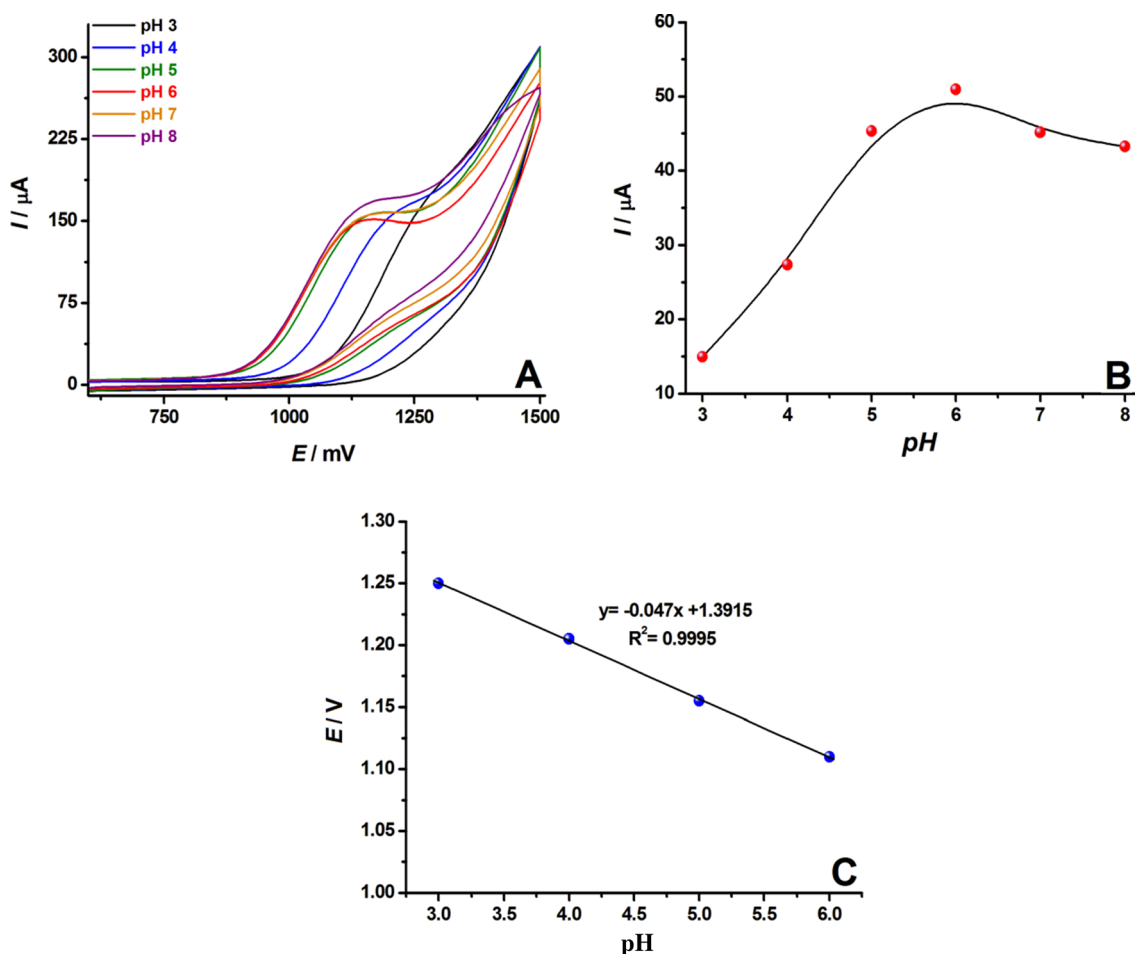
Fig. 3 **A** CVs of 4.0 mM FVP at *f*-MWCNTs/PGE recorded in pH 3–8 BRBS solutions (potential scan range: + 600 - 1500 mV and scan rate: 50 mV/s), the plots of **B** pH–I_a and **C** pH–E_a generated from recorded CVs

both electrodes (Fig. 5C and D). A linear voltammetric response for PGE was obtained between 100 and 500 μM ($I(\mu A) = 0.0110 \times [FVP](\mu M) - 0.4420$; $R^2 = 0.9994$), and this was observed in a wider concentration range of 1.0 to 1500 μM ($I(\mu A) = 0.0153 \times [FVP](\mu M) - 0.0110$; $R^2 = 0.9978$) for *f*-MWCNTs/PGE. To calculate the LOD value, the lowest concentration that gives a voltammetric response was recorded six times. The LOD was calculated according to the equation of 3xSD/m ("SD": the standard deviation for peak currents and "m": the slope calculated from the calibration curve) and determined as 0.27 μM.

The repeatability, reproducibility, and stability parameters were also investigated for *f*-MWCNTs/PGE. The repeatability performance was investigated by recording ten consecutive repeated DPV responses of 100 μM FVP at the same electrode under optimized conditions. The obtained 2.97% relative standard deviation (RSD) value revealed the high repeatability of the designed sensor. The reproducibility was also examined by recording the DPV responses of 100 μM FVP on seven independent electrodes, and the RSD value

of 4.0% supports the good reproducibility of the sensor. The stability of the sensor was examined by recording the inter-day DPV responses of 100 μM FVP on the same electrode on different days, and the decrease in voltammetric response was more than 30% on the second day of use, so it is concluded that the sensor is suitable for only daily use. However, this disadvantage is thought to be tolerable due to the practicality and ease of the preparation of the *f*-MWCNTs/ PGE.

A comparison was made based on analytical performance between the proposed method and similar studies reported in the literature (Table 1). When the studies are examined, various types of composite electrodes and supporting electrolytes are used in combination with different electrochemical methods for the sensitive determination of FVP. However, the high cost of the electrode materials used in the preparation of the related composite electrodes and the laborious and time-consuming cleaning and preparation processes limit the practical usability of the related procedures [1, 3, 6, 9, 16–18, 45]. There is a limit to the number of paper based
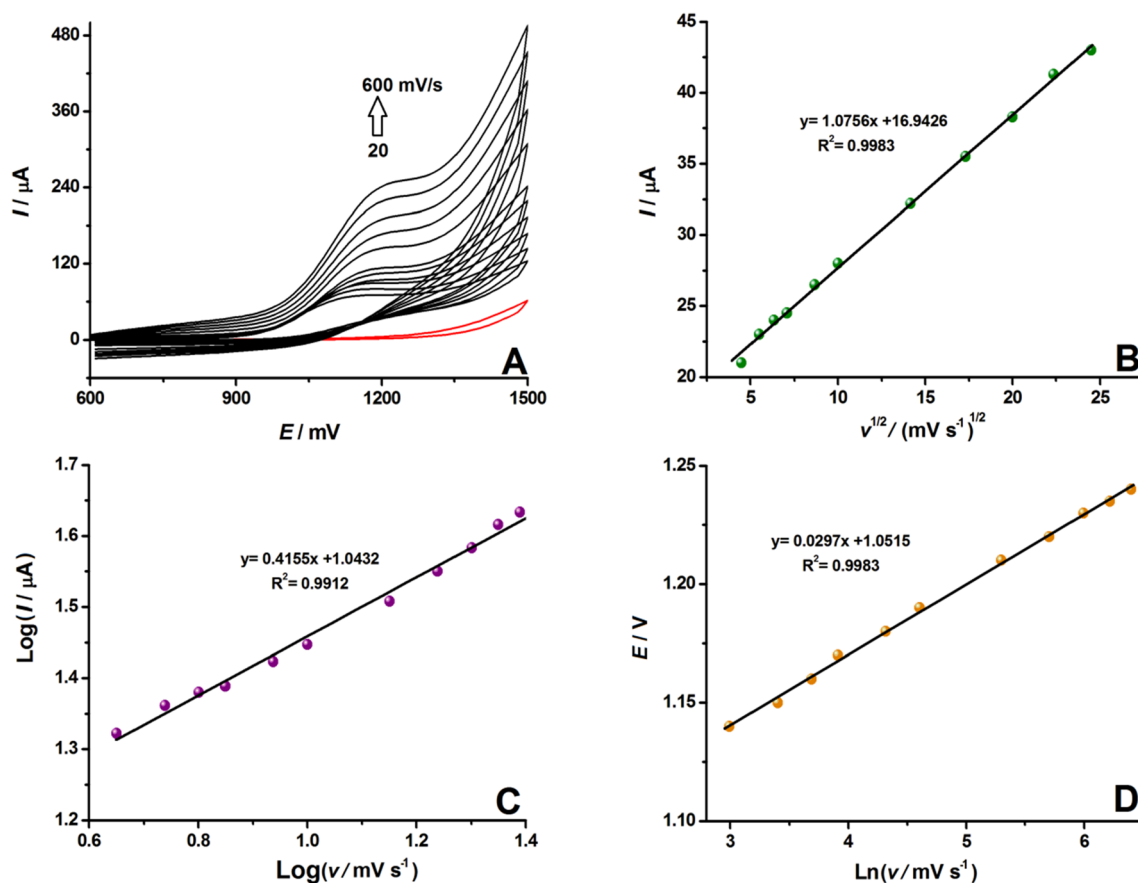
Fig. 4 **A** Recorded CVs (potential scanning range: +600 - +1500 mV; red curve belongs to supporting electrolyte) of pH 6 BRBS containing 4.0 mM FVP at *f*-MWCNTs/PGE at various scan rates (20, 30, 40, 50, 75, 100, 200, 300, 400, 500, and 600 mV/s), **B** I(μA)–$v^{1/2}$, **C** Log$I$–Log$v$ and **D** E_a–ln$v$ plots generated from the recorded CVs

on the use of the PGE in the electrochemical determination of FVP [2, 15]. In addition, the practical preparation process of *f*-MWCNTs/PGE is observed as an advantage in usability. Moreover, the electro-oxidation of FVP at *f*-MWCNTs/PGE occurs at a lower potential, and *f*-MWCNTs/PGE offers a wider linear range for FVP compared to many other studies [1–3, 6, 15–18]. Also, the designed procedure provides a lower LOD than many studies [1, 2, 9, 18]. As a result, the designed method showed comparable and acceptable analytical performance compared with similar studies reported in the literature.

Selectivity for FVP

The selectivity of *f*-MWCNTs/PGE was investigated in the presence of various ionic and molecular species that are likely to be in real samples. The effect of each substance was tested at different interference(Int):FVP ratios according to a certain concentration (100 μM) of the FVP, and the results were given as % changes (with SD) in the oxidation current of the FVP (Table 2). According to the results, 100-fold

ionic (Na$^+$, K$^+$, Mg^{2+}, Ca^{2+}, Zn^{2+}, Al^{3+}, Cl$^-$, NO$_3^-$ ve SO$_4^{2-}$), 100-fold (glucose, fructose, sucrose), 10-fold (dopamine and uric acid) and 1-fold (ascorbic acid) molecular species on the voltammetric response of FVP is considerably lower than the tolerance limit of 10%. It was concluded that the effects of these species on the voltammetric response of FVP are thought to be insignificant. In other words, it has been demonstrated that FVP can be selectively determined at *f*-MWCNTs/PGE in real samples containing these species.

Application to pharmaceutical and biological samples

The feasibility of the method was examined by the application of the sensor to the pharmaceutical tablet, artificial human blood serum, and artificial human urine samples. The FVP content of the pharmaceutical formulation was determined by the combined standard addition-DPV methods, as mentioned before. The FVP amount of pharmaceutical formulation was found to be 201.0 mg per tablet near the labeled value (200 mg) from a pharmaceutical company
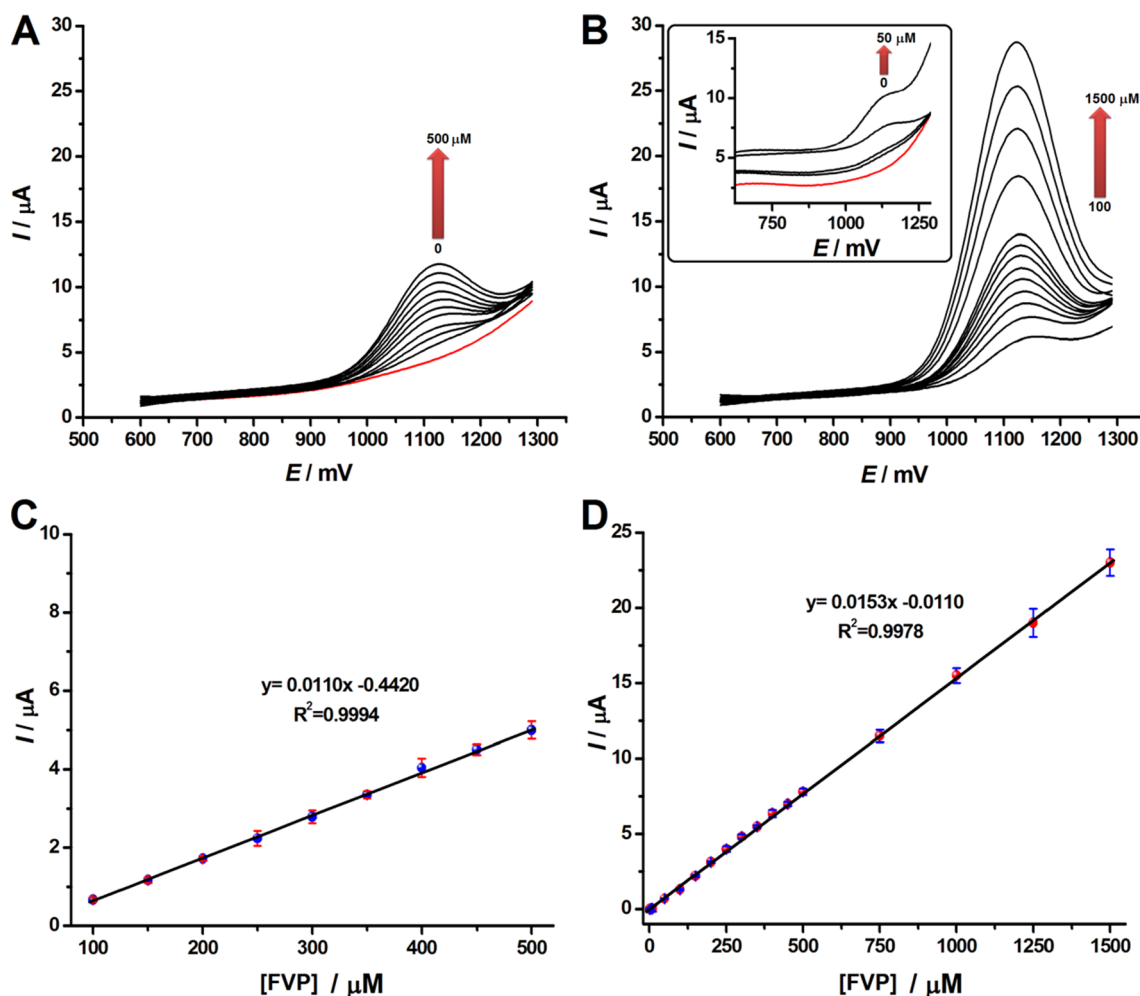
Fig. 5 DPVs recorded for increasing concentrations of FVP at optimized conditions at **A** PGE and **B** *f*-MWCNTs/PGE, the calibration plots for **C** PGE and **D** *f*-MWCNTs/PGE (red curves belongs to supporting electrolyte, $n = 3$)

(Table 3). The recovery method was also applied to the same pharmaceutical formulation and different biological matrices, such as artificial human blood and human urine serums. Following this purpose, various concentrations of FVP were spiked in each sample, and the recovery values were calculated from DPV measurements. The acceptable recovery values (90.2–110.3%) were obtained in different samples (Table 4). All the results proved that the given methodology enables good applicability towards accurate and precise voltammetric quantification of FVP in real and artificial samples prepared in different matrices.

Conclusion

In the presented study, a procedure based on functionalized multi-walled carbon nanotubes modified pencil graphite electrode (*f*-MWCNTs/PGE) was described for the accurate and selective determination of FVP in daily samples.

Compared with traditional solid electrodes like GCE and CPE, PGE provides many advantages such as disposability, availability, low-cost, ease of modification and high electrochemical reactivity in designing electrochemical sensing systems. The combination of the advantageous modifying material, MWCNTs with PGE improves the electrochemical performance based on the voltammetric response of FVP. Moreover, the designed FVP sensor displays acceptable performance based on an extensive linear range (1−1500 µM) with a low LOD (0.27 µM), and high repeatability, reproducibility, and selectivity. The obtained result (201 mg) from the pharmaceutical sample application was so close to the labeled value (200 mg FVP/per tablet), proving that the designed sensor showed an impressive performance in the direct determination of FVP in pharmaceutical formulations. Moreover, the acceptable and satisfactory recovery values (90.2–110.3%) obtained from the application on various samples also demonstrate the high applicability of *f*-MWC-NTs/PGE for accurate and precise quantification of FVP in

Table 1 A Comparsion of the performances of the designed sensor with those of similar studies declared in the literature

Electrode	Method	Response type	Electrolyte	E_a/V	Linear range/μM	LOD/μM	References
[a]CPT/BDD	[h]SW-AdSV	Oxidation	BRBS, pH 8	+1.23	0.064−0.64	0.018	[16]
					0.64−130	0.15	
[b]DNPs/CPE	[i]AdS-SWV	Oxidation	[j]PBS, pH 3	+1.27	0.80−6.0	0.80	[3]
	AdS-DPV	Oxidation		+1.25	0.20−1.0	0.016	
					1.0−5.0	0.673	
[c]MnO$_2$-rGO/SPE	SWV	Oxidation	BRBS, pH 7	+1.23	0.01–55	0.110	[17]
[d]MIP/AuNPs/NiS$_2$NS/BC/GCE	DPV	Oxidation	PBS, pH 8	+1.18	4.2×10^{-4}–1.1	1.3×10^{-4}	[45]
[e]Au@AgCSNPs/PEDOT:PSS/F-MWCNT/GCE	DPV	Oxidation	BRBS, pH 4	+1.23	0.005–0.009	4.6×10^{-4}	[6]
					0.009–1.95		
[f]MoS$_2$@MIP/GCE	DPV	Oxidation	[k]ABS, pH 5	–	1.0×10^{-5}–1.0×10^5	2,0	[9]
[g]GCE	SW-AdSV	Oxidation	BRBS, pH 10	+1.17	6.4−640	1.7	[18]
Pt@rGO/GCE	SWV	Oxidation	BRBS, pH 4	–	3.16−100	2.46	[1]
TbNPs@ poly mTHB[l]/PGE	SWV	Oxidation	PBS, pH 7	+1.14	0.01–0.150	3.1×10^{-3}	[15]
PGE	DPV	Oxidation	BRBS, pH 5	–	5.0–200	1.55	[2]
				–	200–600		
		Reduction		–	1–600	0.35	
f-MWCNTs/PGE	DPV	Oxidation	BRBS, pH 6	+1.13	1−1500	0.27	This work

a: Cathodically pre-treated boron doped diamond electrode, **b**: diamond nanoparticles modified carbon paste electrode, **c**: manganese dioxide-reduced graphene oxide modified screen printed electrode, **d**: molecule printed polymer-gold nanoparticles-nickel sulfide nanosphere-biomass sourced carbon modified glassy carbon electrode, **e**: gold-silver core structured nanoparticles-poly(3,4-ethylenedioxythiophene): poly(styrenesulfonate)-functionalized MWCNTs modified glassy carbon electrode, **f**: molybdenum sulfide-molecul printed polymer modified glassy carbon electrode, **g**: glassy carbon electrode, **h**: square wave-adsorptive stripping voltammetry, **i**: adsorptive stripping voltammetry-square wave voltammetry, **j**: phosphate buffer solution, **k**: acetate buffer solution, **l**: trihydroxybenzene

Table 2 The results obtained from the selectivity studies (stable concentration of FVP = 100 μM and $n = 3$)

Ionic species	Int:FVP ratio	Change in the response of FVP/%	Molecular species	Int:FVP ratio	Change in the response of FVP/%
Na$^+$	100:1	-4.00 ± 1.10	Glucose	100:1	-3.07 ± 0.63
K$^+$	100:1	-1.20 ± 1.65	Fructose	100:1	-3.60 ± 0.36
Mg^{2+}	100:1	-3.07 ± 0.83	Sucrose	100:1	-6.71 ± 0.97
Ca^{2+}	100:1	-3.75 ± 1.02	Dopamine	10:1	-5.10 ± 0.82
Zn^{2+}	100:1	-2.07 ± 0.42	Uric acid	10:1	-3.53 ± 0.96
Al^{3+}	100:1	-3.24 ± 0.46	Ascorbic acid	1:1	-4.00 ± 1.63
Cl$^-$	100:1	-2.76 ± 0.56			
NO$_3^-$	100:1	-2.15 ± 0.88			
SO$_4^{2-}$	100:1	-1.97 ± 0.96			

Table 3 The obtained results from pharmaceutical tablets ($n = 3$)

Sample	FVP content	Found ± SD	RSD/%
FAVIRA® Tablet	200 mg	201.0 ± 3.0 mg	± 1.4

daily samples. It is thought that the designed methodology could potentially be used for routine control and accurate analysis of FVP dosages in drug development units without the use of complicated and long modification procedures, and expensive apparatus.

Materials and methods

Favipiravir (6-fluoro-3-hydroxypyrazine-2-carboxamide, 157.10 g/mol) was supplied from Jiangsu Hansyn Pharmaceutical Co. Ltd. from China. $K_3[Fe(CN)_6]$ was purchased from VWR Chemicals. Uric acid and dopamine were obtained from Alfa Aesar. Multi-walled carbon nanotubes were purchased from DROPSENS. The other reagents of CH_3OH, $K_4[Fe(CN)_6] \cdot 2H_2O$, CH_3COOH, H_3PO_4 (85%), HNO_3 (65%), H_2SO_4 (98%), NaOH, H_3BO_3,

Table 4 The results obtained from recovery studies ($n=3$)

Sample	FVP content/μM	Spiked/μM	Total/μM	Found/μM ± SD	Recovery/%
FAVIRA® tablet	50	0	50	45.7 ± 0.7	91.4 ± 1.6
		25	75	72.0 ± 1.0	96.0 ± 1.2
		50	100	94.8 ± 1.2	94.8 ± 1.2
		75	125	138.0 ± 1.3	110.3 ± 1.1
Artificial blood serum	0	50	50	45.1 ± 0.8	90.2 ± 1.6
		75	75	78.1 ± 1.6	104.1 ± 2.2
		100	100	94.0 ± 1.5	94.0 ± 1.5
Artificial urine serum	0	50	50	47.4 ± 0.9	94.7 ± 1.8
		75	75	77.0 ± 2.2	102.0 ± 3.0
		100	100	93.0 ± 1.6	93.0 ± 1.6

KCl, NaCl, NaCH$_3$COO•3H$_2$O, KNO$_3$, Na$_2$SO$_4$, Na$_2$CO$_3$, MgCl$_2$, CaCl$_2$•2H$_2$O, Zn(NO$_3$)$_2$, Al(NO$_3$)$_3$, *L*-ascorbic acid, *D*-glucose, sucrose, and *D*-fructose used in the study were purchased from Sigma-Aldrich, Isolab, and Merck companies. Britton Robinson buffer solution (BRBS) was prepared by mixing appropriate volumes of an acidic solution (containing 0.4 M CH$_3$COOH, H$_3$PO$_4$, H$_3$BO$_3$, and 0.1 M KCl) and a basic solution (containing 0.2 M NaOH and 0.1 M KCl) under the control of a pH meter.

The ultra-pure water required for the preparation of the solutions was supplied by an Elga Option Q7B water purification system with 18.2 MΩ cm^{-1} resistance. A Hanna HI 221 pH meter with a combined glass electrode was used for the preparation of buffer solutions. Electrochemical measurements were carried out using a Galvanoplot brand GX203 model compact potentiostat (Turkey) device. A conventional three-electrode system was used for electrochemical measurements. In this system, the working electrode is TOMBOW 2B 0.5 mm (Japan) pencil leads; the reference electrode is BASI brand ALS 013,429 RE-1CP model Ag/AgCl$_{(sat. KCl)}$ and the auxiliary electrode is: the following BASI brand MW-1033 model Pt wire. In all electrochemical measurements, a length of 1.0 cm of the working electrode (equal to the geometric area of 0.159 cm^2) was used. The surface characterizations of electrodes were performed by a JEOL JSM-7100-F scanning electron microscopy (SEM) device at Çanakkale Onsekiz Mart University Science and Technology Application and Research Center (ÇOBİLTUM).

Functionalization of MWCNTs and preparation of the *f*-MWCNTs/PGE

Acidic functionalization of MWCNTs was performed using a procedure given in the literature [47]. For this purpose, 1.0 g of MWCNTs was transferred to the HNO$_3$: H$_2$SO$_4$ solution prepared with a 3:1 (v/v) ratio and mixed for 1 h at room temperature. At the end of this period, the resulting suspension was filtered, and the solid part was washed abundantly with distilled water and filtered again. This process was continued until the pH of the filtrate reached neutral. Afterward, the solid part was separated by filtration, kept in an oven at 80 °C for 5 h, and left to dry. The resulting precipitate was termed as "*f*-MWCNTs".

2.0 mg/mL *f*-MWCNTs solution was prepared in dimethyl formamide (DMF), and *f*-MWCNTs/PGE was prepared by immersing pencil lead in this solution and drying it under an infrared lamp. The immersion time and immersion number in the preparation step were optimized by the CV method, and the optimum conditions for these parameters were found to be 60 s and two (2) times, respectively.

Electrochemical measurements

The electrochemical characterizations of PGE and *f*-MWCNTs/PGE were realized by recording CVs (at a scan rate of 50 mV/s and a potential range of + 500 to + 1200 mV) and EI (frequency range: 100,000–0.10 Hz) curves of 0.1 M KCl solution containing 5.0 mM K$_4$[Fe(CN)$_6$]/K$_3$[Fe(CN)$_6$] redox couple (Fe(CN)$_6^{3-/4-}$). The electrochemical behavior of 4.0 mM and 100 μM FVP prepared in pH 6 BRBS at modified and bare electrodes was examined by CV and DPV methods, respectively. Optimum conditions for the parameters affecting the differential pulse voltammetric response of FVP, such as step potential (E_{Step}) and pulse amplitude (E_{Amp}), were determined by recording the voltammetric responses of pH 6 BRBS containing 50 μM FVP at *f*-MWCNTs/PGE under different E_{Step} and E_{Amp} conditions. The optimum conditions for these parameters were determined to be 5 mV and 10 mV, respectively.

Application on real samples

The feasibility of the proposed procedure was examined using both standard addition and recovery methods. A pharmaceutical formulation in tablet form (FAVIRA®)

containing 200 mg FVP was supplied from a local pharmacy. Artificial blood serum [48] and artificial urine serum [49] samples were prepared according to the procedures described in the literature.

The FVP content of FAVIRA® was directly determined by DPV using the standard addition method. For this purpose, a tablet was dissolved in 10 mL of DMF and the resulting solution was diluted in a ratio of 1:1000 with pH 6 BRBS in an electrochemical cell, and DPV was recorded. Then, standard additions were made to the standard FVP solution (10^{-2} M) and voltammograms were recorded similarly. The FVP content of the tablet was calculated by subtracting a calibration curve.

Also, the recovery studies were performed with FAVIRA® tablets, artificial blood, and artificial urine samples. For this purpose, known concentrations of FVP were spiked into each sample, and then the standard additions were made by recording the voltammograms, and recoveries were calculated.

References

1. Bouali W, Erk N, Kholafazadehastamal G, Naser M, Tiris G (2023) Diam Relat Mater 131:109609
2. Erşan T, Dilgin DG, Kumrulu E, Kumrulu U, Dilgin Y (2023) Electroanalysis 35:e202200295
3. Kanbeş Dindar Ç, Bozal-Palabiyik B, Uslu B (2022) Electroanalysis 34:1174
4. World Health Organization (WHO) Coronavirus (COVID-19) Dashboard (2023) https://covid19.who.int/ Accessed: 2 Apr 2023
5. Liu X, Liu C, Liu G, Luo W, Xia N (2020) Theranostics 10:7821
6. El-Wekil MM, Hayallah AM, Abdelgawad MA, Abourehab MA, Shahin RY (2022) J Electroanal Chem 922:116745
7. Madelain V, Mentré F, Baize S, Anglaret X, Laouénan C, Oestereich L, Nguyen THT, Malvy D, Piorkowski G, Graw F (2020) CPT: Pharmacomet Syst Pharmacol 9:258
8. Habler K, Brügel M, Teupser D, Liebchen U, Scharf C, Schönermarck U, Vogeser M, Paal M (2021) J Pharm Biomed Anal 196:113935
9. Wang S, Wang C, Xin Y, Li Q, Liu W (2022) Microchim Acta 189:125
10. Bulduk İ (2021) Acta Chromatogr 33:209
11. Megahed SM, Habib AA, Hammad SF, Kamal AH (2021) Spectrochim Acta A Mol Biomol Spectrosc 249:119241
12. Nazifa Sabir AS, Mobina L, Mehfuza M, Seema P, Ahmed A, Khan JG (2021) J Pharm Res Int 33:254
13. Koçak ÇC, Aslışen B, Karabiberoğlu Ş, Özdokur KV, Aslan A, Koçak S (2022) ChemistrySelect 7:e202201864
14. Dedelaite L, Kizilkaya S, Incebay H, Ciftci H, Ersoz M, Yazicigil Z, Oztekin Y, Ramanaviciene A, Ramanavicius A (2015) Colloids Surf A: Physicochem Eng Asp 483:279
15. Ali MF, Saraya RE, El Deeb S, Ibrahim AE, Salman BI (2023) Biosensors 13:243
16. Allahverdiyeva S, Yunusoglu O, Yardım Y, Şentürk Z (2021) Anal Chim Acta 1159:338418
17. Mohamed MA, Eldin GM, Ismail SM, Zine N, Elaissari A, Jaffrezic-Renault N, Errachid A (2021) J Electroanal Chem 895:115422
18. Akca Z, Özok Hİ, Yardim Y, Şentürk Z (2022) Turk J Chem 46:869
19. Prasertying P, Yamkesorn M, Chimsaard K, Thepsuparungsikul N, Chaneam S, Kalcher K, Chaisuksant R (2020) J Sci-Adv Mater Devices 5:330
20. Trnkova L, Triskova I, Cechal J, Farka Z (2021) Electrochem Commun 126:107018
21. Riman D, Rozsypal J, Halouzka V, Hrbac J, Jirovsky D (2020) Microchem J 154:104606
22. David IG, Popa DE, Buleandra M (2017) J Anal Methods Chem 2017:1905968
23. Navratil R, Kotzianova A, Halouzka V, Opletal T, Triskova I, Trnkova L, Hrbac J (2016) J Electroanal Chem 783:152
24. Riman D, Prodromidis MI, Jirovsky D, Hrbac J (2019) Sens Actuators B Chem 296:126618
25. Torrinha Á, Amorim CG, Montenegro Maria CBSM, Araújo AN (2018) Talanta 190:235
26. Huang YY, Pang YH, Shen XF, Jiang R, Wang YY (2022) Talanta 236:122859
27. Naik TSK, Kesavan AV, Swamy BK, Singh S, Anil AG, Madhavi V, Ramamurthy PC (2022) Mater Chem Phys 278:125663
28. Ishtiaq S, Sohail M, Rasul S, Zia AW, Siller L, Chotana GA, Sharif M, Nafady A (2022) ACS Appl Nano Mater 5:14336
29. Sedhu N, Kumar JJ, Sivaguru P, Raj V (2023) J Electroanal Chem 928:117037
30. Zambrano-Intriago LA, Amorim CG, Araújo AN, Gritsok D, Rodríguez-Díaz JM, Montenegro MC (2023) Sci Total Environ 855:158865
31. Carvalho RM, Pedão ER, Guerbas FMR, Tronchini MP, Ferreira VS, Petroni JM, Lucca BG (2023) Talanta 252:123873
32. Yıldız C, Bayraktepe DE, Yazan Z (2022) ChemistrySelect 7:e202201697
33. Heydari H, Gholivand MB, Abdolmaleki A (2016) Mater Sci Eng C 66:16
34. Dalkiran B, Brett CM (2022) Microchem J 179:107531
35. Gong ZQ, Sujari ANA, Ab Ghani S (2012) Electrochim Acta 65:257
36. Kolahi-Ahari S, Deiminiat B, Rounaghi GH (2020) J Electroanal Chem 862:113996
37. Manjunatha P, Nayaka YA, Chethana BK, Vidyasagar CC, Yathisha RO (2018) Sens Bio-Sens Res 17:7
38. Ali AMBH, Rageh AH, Abdelaal FA, Mohamed AMI (2023) Microchem J 185:108261
39. Abedini S, Rafati AA, Ghaffarinejad A (2022) New J Chem 46:20403
40. Feng J, Deng P, Xiao J, Li J, Tian Y, Wu Y, Liu J, Li G, He Q (2021) J Food Compos Anal 96:103708
41. Afkhami A, Bahiraei A, Madrakian T (2016) Mater Sci Eng C 59:168
42. Alothman ZA, Bukhari N, Wabaidur SM, Haider S (2010) Sens Actuators B Chem 146:314
43. Zhu YH, Zhang ZL, Pang DW (2005) J Electroanal Chem 581:303
44. Erk N, Mehmandoust M, Soylak M (2022) Biosensors 12:769
45. Mehmandoust M, Khoshnavaz Y, Tuzen M, Erk N (2021) Microchim Acta 188:434

46. Laviron E (1974) J Electroanal Chem 52:355
47. Güneş M, Karakaya S, Dilgin Y (2022) Electroanalysis 34:1644
48. Özcan HM, Sezgintürk MK (2015) Biotechnol Prog 31:815
49. Sarigul N, Korkmaz F, Kurultak İ (2019) Sci Rep 9:20159